Choline transport links macrophage phospholipid metabolism and inflammation

Received for publication, March 27, 2018, and in revised form, May 29, 2018 Published, Papers in Press, June 7, 2018, DOI 10.1074/jbc.RA118.003180

Shayne A. Snider[‡§1,2], Kaitlyn D. Margison[‡§1], Peyman Ghorbani[‡§], Nicholas D. LeBlond[‡§3], Conor O'Dwyer[‡§], Julia R. C. Nunes[‡§], Thao Nguyen[‡§¶], Hongbin Xu[‡§¶], Steffany A. L. Bennett[‡§¶], and Morgan D. Fullerton[‡§4]

From the [‡]University of Ottawa Centre for Infection, Immunity, and Inflammation and Centre for Catalysis Research and Innovation, the [¶]Ottawa Institute of Systems Biology and University of Ottawa Brain and Mind Institute, and the [§]Department of Biochemistry, Microbiology, and Immunology, Faculty of Medicine, University of Ottawa, Ottawa, Ontario K1H 8M5, Canada

Edited by Luke O'Neill

Choline is an essential nutrient that is required for synthesis of the main eukaryote phospholipid, phosphatidylcholine. Macrophages are innate immune cells that survey and respond to danger and damage signals. Although it is well-known that energy metabolism can dictate macrophage function, little is known as to the importance of choline homeostasis in macrophage biology. We hypothesized that the uptake and metabolism of choline are important for macrophage inflammation. Polarization of primary bone marrow macrophages with lipopolysaccharide (LPS) resulted in an increased rate of choline uptake and higher levels of PC synthesis. This was attributed to a substantial increase in the transcript and protein expression of the choline transporter-like protein-1 (CTL1) in polarized cells. We next sought to determine the importance of choline uptake and CTL1 for macrophage immune responsiveness. Chronic pharmacological or CTL1 antibody–mediated inhibition of choline uptake resulted in altered cytokine secretion in response to LPS, which was associated with increased levels of diacylglycerol and activation of protein kinase C. These experiments establish a previously unappreciated link between choline phospholipid metabolism and macrophage immune responsiveness, highlighting a critical and regulatory role for macrophage choline uptake via the CTL1 transporter.

Macrophages represent a diverse and plastic subset of phagocytic innate immune cells that are critically important for immune surveillance and tissue homeostasis. *In vivo*, macrophage phenotypes are almost exclusively driven by external stimuli that dictate the activation of necessary cellular programs (1, 2). In the context of infection or pro-inflammatory stimuli, macrophages evoke a wave of cellular responses, including the production and secretion of cytokines as well as membrane biogenesis and phagocytosis. These processes are intricately linked to phospholipid homeostasis; however, there are few papers linking phospholipid metabolism and macrophage biology.

Choline is a quaternary amine and essential nutrient that participates in acetylcholine synthesis (cholinergic neurons) and one-carbon metabolism (primarily thought to be in the liver and kidney). However, in eukaryotic nonneuronal cells, choline is predominantly used for the synthesis of phosphatidylcholine (PC),[5] the major outer-leaflet phospholipid. Once inside the cell, choline is shuttled along the Kennedy pathway (3) and combined with diacylglycerol (DAG) to form PC at the ER membrane. Moreover, PC can also be degraded by numerous phospholipases to yield lipid intermediates that can then be recycled or further processed. Although under most conditions, the CTP:phosphocholine cytidylyltransferase (CCT) or DAG availability has been shown to control flux through the Kennedy pathway (4), recent studies have begun to shed light on the potential regulation of this pathway by choline transporters (5–7).

Due to its positive charge, specialized transporters facilitate cellular choline uptake. High-affinity transport exists in cholinergic neurons (via CHT1/Slc5a7) (8, 9), whereas members of the organic cation transporter family (OCT/Slc22a1–20) are generic transporters of heavy metals and organic cations that have a low rate and specificity for transporting choline (10, 11). Another family of choline transporters has been identified and named the choline transporter-like proteins (CTL1–5). CTL1 is

This work was supported by Natural Science and Engineering Research Council (NSERC) of Canada Discovery Grants RGPIN-2015-04004 (to M. D. F.) and RGPIN-2015-5377 (to S. A. L. B.) and Canadian Institutes of Health Research Grant MOP 311838 (to S. A. L. B.). The authors declare that they have no conflicts of interest with the contents of this article.

This article contains Figs. S1–S6.

[1] Both authors contributed equally to this work.

[2] Supported by an NSERC Canadian Graduate Scholarship.

[3] Supported by an Ontario Graduate Scholarship.

[4] Supported by Canadian Institutes of Health Research New Investigator Award MSH141981 and recipient of an Ontario Ministry of Research, Innovation, and Science Early Researcher Award. To whom correspondence should be addressed: Dept. of Biochemistry, Microbiology, and Immunology, Faculty of Medicine, University of Ottawa, 4109A Roger Guindon Hall, 451 Smyth Rd., Ottawa, Ontario K1H 8M5, Canada. Tel.: 613-562-5800 (ext. 8310); E-mail: morgan.fullerton@uottawa.ca.

[5] The abbreviations used are: PC, phosphatidylcholine; CTL1, choline transporter-like protein 1; CTL1-Ab, CTL1-specific primary antibody; DAG, diacylglycerol; PKC, protein kinase C; CCT, phosphocholine cytidylyltransferase; CHT1, high-affinity choline transporter; OCT, organic ion transporter; LPS, lipopolysaccharide; M[0], basal macrophage; M[LPS], LPS-stimulated macrophage; AA, arachidonic acid; SM, sphingomyelin; ESI, electrospray ionization; TG, triglyceride; BMDM, bone marrow-derived macrophage(s); *Pcyt1*, gene encoding phosphocholine cytidylyltransferase; *Pcyt2*, gene encoding phosphoethanolamine cytidylyltransferase; HC3, hemicholinium-3; TNF, tumor necrosis factor; IL, interleukin; BIM, bisindolylmaleimide I; SRM, selected reaction monitoring; IDA, information-dependent acquisition; EPI, enhanced product ion; ER, endoplasmic reticulum; AA, arachidonic acid; DAPI, 4′,6-diamidino-2-phenylindole; RT, room temperature; ANOVA, analysis of variance.

ubiquitously expressed and is thought to be primarily responsible for mediating choline uptake in nonneuronal cells (5, 6, 12–16). Although few studies have investigated choline metabolism in immune cells, early experiments revealed that macrophage stimulation with the bacterial endotoxin lipopolysaccharide (LPS) acutely increased PC synthesis (17, 18). When PC synthesis was compromised by myeloid-specific deletion of CCTα (the rate-limiting enzyme in PC synthesis), cells had a reduced capacity to secrete pro-inflammatory cytokines in response to LPS (19). These data suggest that in response to an inflammatory insult, choline availability and PC synthesis may be important.

In the present study, we sought to investigate how macrophage LPS polarization affects choline uptake and subsequent metabolism. We observed an increase in PC synthesis in response to LPS due to an up-regulation in the transcription of the CTL1 gene (*Slc44a1*), which facilitates an increased rate of uptake and synthesis of PC. Conversely, we also sought to ask the reciprocal question of how limiting the availability of choline might affect acute response to LPS stimulation. Pharmacological and antibody-mediated inhibition of CTL1 limited choline uptake and diminished PC content, which altered cytokine secretion. Interestingly, we found that inhibition of PC synthesis resulted in an increase in DAG accumulation and subsequent protein kinase C (PKC) activation. Restoring PC levels and inhibiting PKC activity were important for regulating the pro-inflammatory responses, linking macrophage phospholipid metabolism and inflammation.

Results

Macrophage LPS stimulation increases choline uptake and alters PC homeostasis

LPS is known to increase choline incorporation into PC (17, 18); however, the effect of long-term exposure to LPS on choline uptake and metabolism remains unclear. Bone marrow–derived macrophages (BMDM) were treated for 48 h with LPS, and the transcript expression of pro-inflammatory (*Tnfa*, *Il1b*, *Il6*, and the ratio of *iNos/Arg1*) or anti-inflammatory (*Tgfb1* and *Mrc1*) markers was measured to confirm polarization (Fig. S1). The rate of choline uptake was markedly increased in M[LPS] compared with control M[0] (Fig. 1*A*). Moreover, LPS-polarization increased the maximal transport of choline from 418 ± 49 to 821 ± 62 pmol/mg/min, where the apparent affinity remained unchanged (68.62 ± 20.07 to 72.66 ± 13.42 μM) (Fig. 1*B*).

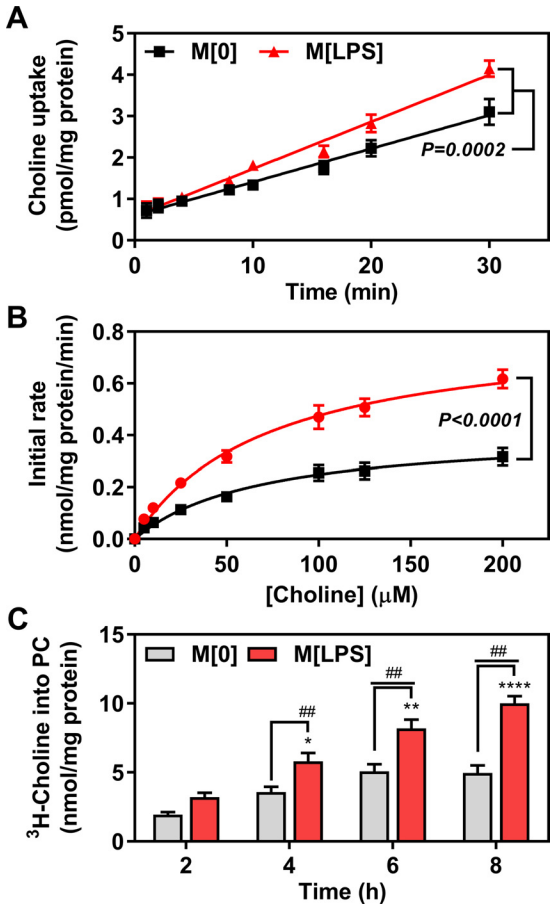

Figure 1. LPS stimulation increases choline uptake and PC synthesis. BMDM were treated with LPS (100 ng/ml) for 48 h before measuring choline uptake. *A*, choline uptake was measured at the indicated times by incubating cells in a solution of KRH buffer containing 1 μCi/ml [^{3}H]choline chloride (n = 6 separate bone marrow isolations, each performed in triplicate). *B*, choline uptake was measured over 10 min by incubating cells in a solution of KRH buffer containing 1 μCi/ml [^{3}H]choline chloride and increasing amounts of nonradiolabeled "cold" choline (n = 6–8 separate bone marrow isolations, each performed in triplicate). Choline uptake was determined by measuring intracellular radioactivity, which was plotted against the amount of protein. *C*, BMDM were treated with LPS (100 ng/ml) for 48 h before treatment with 1 μCi/ml [^{3}H]choline chloride in DMEM for the indicated times, and the incorporation into PC was determined (n = 6–9 separate bone marrow isolations, each performed in triplicate). Data are expressed as mean ± S.E. (*error bars*). The rates of choline uptake (*A*) were determined via linear regression, where the p value indicated represents significance between M[0] and M[LPS] cells. For choline uptake kinetics (*B*), data were fit to the Michaelis–Menten curve, and statistical significance is represented as follows: ****, $p < 0.0001$, as determined by a comparison of the curve fit using extra sum-of-squares F-test. For PC synthesis (*C*), statistical significance is represented as follows: *, $p < 0.05$; **, $p < 0.01$; ****, $p < 0.0001$ compared between treatments; ##, $p < 0.01$ compared with the 2-h time point determined by two-way ANOVA.

Following uptake in nonhepatic or renal tissue, choline is rapidly phosphorylated and shuttled along the CDP-choline pathway to produce PC. In keeping with an increased rate of uptake, the incorporation of [^{3}H]choline into PC was higher in LPS-stimulated macrophages (Fig. 1*C*). It has been shown previously that arachidonic acid (AA) liberated from PC via the actions of phospholipase A2 can have subsequent roles in inflammatory signaling via conversion to prostaglandin and lipid mediators following LPS stimulation (17, 20, 21). We reasoned that perhaps LPS stimulation of PC synthesis might be accompanied by a coordinated increase in overall PC turnover to facilitate AA metabolism. However, pulse-chase experiments revealed no difference in the rate of PC degradation between M[LPS] and M[0] cells (Fig. S2*A*). There was also no difference in the sensitivity to the choline uptake inhibitor hemicholinium-3 (HC3) between naive and LPS-treated cells (Fig. S2*B*). These data indicate that when chronically polarized with LPS, choline transport and subsequent incorporation into PC are up-regulated.

To validate these findings and address directly whether the levels of PC and/or the downstream lipid sphingomyelin (SM) were increased following LPS stimulation, we used a targeted lipidomic approach to profile and quantify total content and lipid species at the molecular level. A total of 35 PC and 27 SM

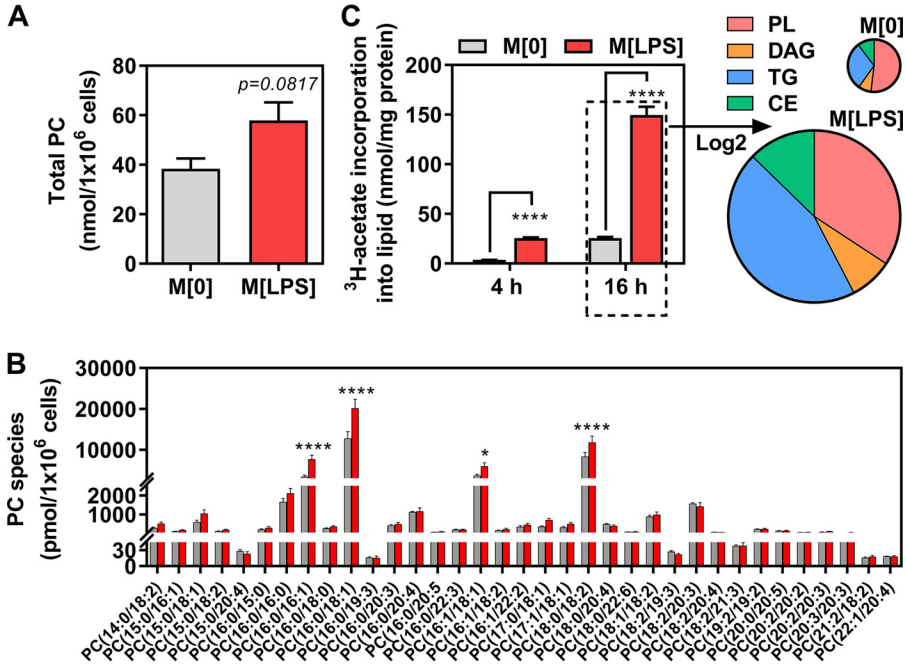

Figure 2. Macrophage LPS-polarization increases PC and *de novo* lipogenesis. BMDM were treated with or without LPS (100 ng/ml) for 48 h. HPLC-ESI-MS/MS lipidomics was used to assess total PC content (*A*) and PC fatty acid composition (*B*) ($n = 3$ separate bone marrow isolations). Cells treated with and without LPS were incubated in the presence of [^{3}H]acetate to measure fatty acid synthesis, where *C* is the incorporation into all lipids, with the proportional incorporation of [^{3}H]acetate-derived fatty acids into phospholipid (*PL*), DAG, TG, or cholesteryl ester (*CE*) shown to the *right*. Data for *A–C* are expressed as mean ± S.E. (*error bars*), where statistical significance is represented as follows: *, $p < 0.05$; ****, $p < 0.0001$ compared with M[0]-treated cells as determined by two-way ANOVA as indicated. For *D*, M[LPS] is shown relative to M[0], where the $\log_2$-transformed relative difference is reflected by the *size* of the *pie* ($n = 4$ separate bone marrow isolations, each performed in triplicate).

species were detected by HPLC electrospray ionization tandem MS (HPLC-ESI-MS/MS). Corroborating recent work in murine immortalized macrophages (22), we found that in LPS-treated macrophages, total PC content was increased ~50% (Fig. 2*A*) ($p = 0.0817$, using a small sample size of $n = 3$). There was a trend consistent with higher levels of SM in LPS-treated cells, although side-chain composition was only different between treatments in SM(d18:1/16:0) (Fig. S3, *A* and *B*). However, there was a significant increase in the most abundant PC molecular species, including PC(16:0/16:1), PC(16:0/18:1), PC(16:1/18:1), and PC(18:0/18:2) (Fig. 2*B*), which represent potentially newly synthesized, desaturated, and elongated fatty acids. The transcript expression of *Elovl6* and *Scd1*, which encode for the elongase and desaturase activity, respectively, were up-regulated by 48-h LPS treatment (Fig. S3*C*). To further investigate this phenomenon, we measured LPS-stimulated *de novo* fatty acid synthesis by assessing the incorporation of [^{3}H]acetate into all lipids, which was increased overall (Fig. 2*C*) and confirms previously published work (23). Interestingly, despite the dramatic increase in [^{3}H]acetate-derived fatty acids and an absolute increase in PC, the relative proportion of *de novo* fatty acids incorporated into the total phospholipid pool diminishes with LPS treatment compared with control (51.73% *versus* 36.55%; $p < 0.01$). As reported previously (24, 25), LPS triggered an increased fatty acid incorporation into triglyceride (TG) (29.89% *versus* 45.09%; $p < 0.0001$), where fatty acid esterification onto DAG or cholesteryl esters remained consistent between naive and LPS-treated macrophages (Fig. 2*C*). Together, these results demonstrate that chronic LPS polarization stimulates an increase in total PC and a remodeling of fatty acid side chains, potentially in keeping with augmented lipogenesis observed with 48-h LPS-polarized cells.

The choline transporter CTL1 is up-regulated in LPS-stimulated macrophages

We hypothesized that the protein expression of choline transporters was increased in LPS-stimulated cells, which would explain the observed increase in the maximal rate of choline transport. We first assessed the transcript levels of the potential choline transport proteins (choline transporter-like proteins *Slc44a1–5*, organic cation transporters *Slc22a1–3*, and the high-affinity choline transporter *Slc5a7*) and show that only *Slc44a1*/CTL1 and *Slc44a2*/CTL2 were expressed in BMDM (Fig. 3) (data not shown). In response to chronic LPS stimulation, the transcript expression of *Slc44a1* and *Slc44a2* was significantly increased compared with untreated cells (Fig. 3*A*). There were no differences in transcript expression of the first two enzymes in the CDP-choline pathway, *Chka* or *Pcyt1*, or the rate-limiting enzyme of the CDP-ethanolamine pathway, *Pcyt2* (Fig. 4*A*). Interestingly, although there was a corresponding up-regulation of the CTL1 protein with LPS stimulation, CTL2 protein expression was unchanged (Fig. 3*B*). This was counter to the increased *Slc44a2* transcript expression and suggests that CTL1 is the main choline transporter in BMDM. Taken together, these results demonstrate that in response to chronic stimulation with LPS, the transcript and protein expression of CTL1 is correspondingly higher and may facilitate the increase in choline metabolism fueled by inflammatory stimulation.

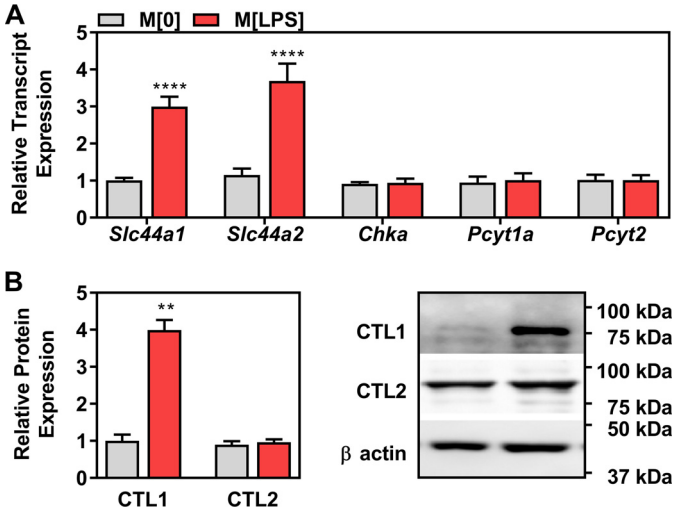

Figure 3. Choline transporter transcript and protein expression induced by LPS. BMDM were treated with LPS (100 ng/ml) for 48 h. *A*, qPCR determination of the relative expression of *Slc44a1*, *Slc44a2*, *Chka*, *Pcyt1a*, and *Pcyt2*, which were normalized to the average expression of *β-actin* and *Tbp* ($n = 4$ separate bone marrow isolations, each performed in triplicate). Data are mean ± S.E. (*error bars*), where statistical significance is represented as follows: ****, $p < 0.0001$ compared with M[0] cells as determined by an unpaired two-tailed Student's *t* test. *B*, protein expression of CTL1 and CTL2 was determined and normalized to β-actin ($n = 3$ separate bone marrow isolations, each run in duplicate). Data are mean ± S.E. of the densitometry quantification (ImageJ), and the blots are representative images of the biological replicates, where statistical significance is represented as follows: **, $p < 0.01$ compared with M[0] cells as determined by an unpaired two-tailed Student's *t* test.

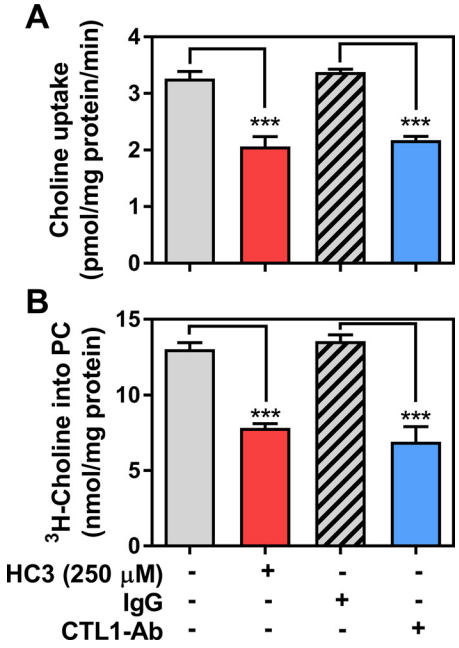

Figure 4. Chronic pharmacological or CTL1-specific antibody inhibition lowers choline uptake and PC levels. BMDM were incubated for 48 h in the presence or absence of the choline uptake inhibitor HC3 (250 μM), where DMSO was used as a vehicle control or with a primary CTL1 antibody, where an isotype control IgG antibody was used (both at 1:250 dilution). *A*, acute [^{3}H]choline uptake was assessed over 10 min ($n = 4$ separate isolations, each performed in triplicate). *B*, chronic choline uptake inhibition was accompanied by chronic [^{3}H]choline incorporation into PC ($n = 4$ separate isolations, each performed in triplicate). Data are mean ± S.E. (*error bars*), where statistical significance is represented as follows: ***, $p < 0.001$ compared with control treatment as indicated and assessed by one-way ANOVA.

Chronic inhibition of choline uptake lowers PC

Whole-body choline deficiency manifests symptoms of fatty liver and muscle fatigue (26); however, the effects of choline depletion on macrophages are not known. To address this question, we used a pharmacological and antibody occlusion approach to chronically inhibit general and CTL1-specific choline uptake. Following a chronic (48-h) incubation with either the choline uptake inhibitor HC3 or a CTL1-specific primary antibody (CTL1-Ab), choline uptake was significantly reduced (Fig. 4*A*). Next, we treated macrophages with either HC3 or the CTL1-Ab in the presence of [^{3}H]choline for 48 h to assess the endogenous pool of PC after the duration of choline uptake inhibition. In keeping with the choline uptake measurements, the amount of PC was significantly reduced in both HC3 and CTL1-Ab–treated cells (Fig. 4*B*). HC3-mediated choline uptake inhibition was equal to that of the CTL1-specific antibody, suggesting that CTL1 is the primary transporter of choline in these cells. Chronic treatment at the indicated concentrations of HC3 had no affect on cell size and slightly but significantly decreased cell viability (Fig. S4). These effects were not observed using the CTL1-Ab (data not shown).

Chronic inhibition of choline uptake alters cytokine secretion

Previous work has shown that CCTα-deficient macrophages, which lack the rate-limiting enzyme in the CDP-choline pathway and have reduced PC content, secrete less TNFα and IL-6 in response to LPS. This is due to secretory defects at the level of the ER and Golgi. In our BMDM model of choline uptake inhibition, we used a cytokine array panel and determined that chronic HC3 treatment altered 6-h LPS-stimulated secretion of various cytokines and chemokines, including TNFα and IL-10 (Fig. S5). Contrary to the findings in CCTα-deficient cells, when we assessed LPS-stimulated primary macrophages that had experienced chronic choline uptake inhibition (6-h LPS), we observed a significant increase in the secretion of both TNFα and IL-6, along with significant reductions in IL-10 secretion (Fig. 5, *A–C*), whereas no differences in IL-1β were seen (data not shown). The affect of choline uptake inhibition was only noted in the presence of LPS (Fig. 5, *A–C*).

Inhibition of choline uptake increases DAG and PKC activation

The final step in the biosynthesis of PC involves the combination of CDP-choline and DAG at the ER. We next tested the hypothesis that the inhibition of choline uptake subsequently altered the levels or metabolism of DAG. We incubated BMDM with either HC3 or the CTL1-Ab in the presence of [^{3}H]glycerol for 48 h and demonstrated that in response to both forms of inhibition, there was a marked increase in the amount of DAG (Fig. 6*A*). In addition, there was a significant increase in TG levels (Fig. 6*B*) and, as expected, a significant reduction in [^{3}H]glycerol incorporation into PC (Fig. 6*C*). In keeping with altered DAG metabolism, HC3 treatment resulted in an increase in the transcript expression of the final step of TG synthesis, *Dgat2*, but not *Dgat1* (Fig. 6*D*). This was associated with more defined lipid droplets in HC3-treated cells (Fig. 6*E*). Increased cellular DAG is known to activate conventional and novel isoforms of PKC, which in turn has been linked to macrophage inflammation (27–29). HC3-mediated chronic choline

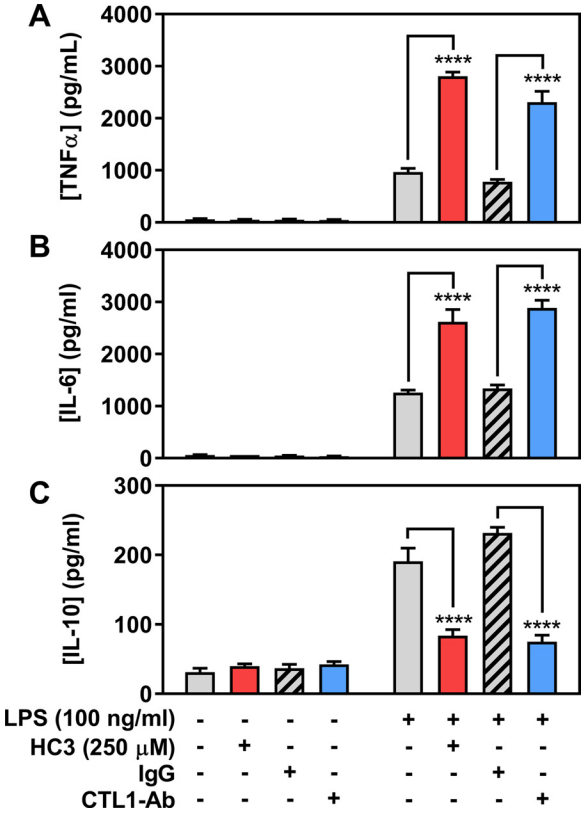

Figure 5. Inhibiting choline uptake alters LPS-induced cytokine secretion. Cells were incubated in the presence or absence of HC3 (250 μM) or CTL1-Ab (1:250) for 48 h. The medium was removed, and cells were stimulated with 100 ng/ml LPS for 6 h (with inhibitor treatments replenished), and from the supernatant, TNFα (*A*), IL-6 (*B*), and IL-10 secretion (*C*) were determined ($n = 5$ separate isolations, each performed in triplicate). Data are mean ± S.E. (*error bars*), where statistical significance is represented as follows: ****, $p < 0.0001$ compared with LPS-stimulated control treatment, as indicated, assessed by two-way ANOVA.

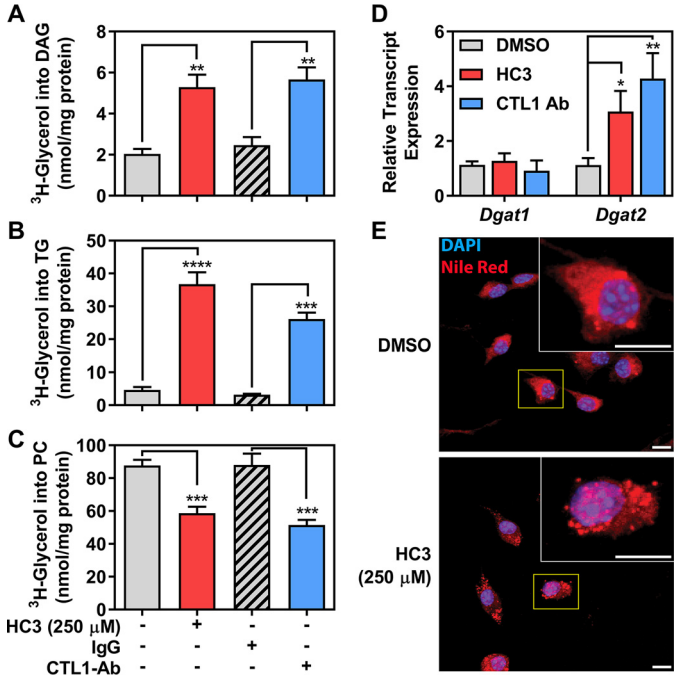

Figure 6. Inhibiting choline uptake causes accumulation and redirection of DAG. BMDM were pulsed with [^{3}H]glycerol for 48 h in the presence or absence of choline uptake inhibitor HC3 (250 μM) or the CTL1-Ab (1:250). Lipids were then extracted and separated via TLC to determine radioactivity of DAG (*A*), TG (*B*), and PC (*C*) ($n =$ at least 4 separate isolations). *D*, qPCR determination of the relative expressions of Dgat1 and Dgat2 after 48-h treatment, as indicated, which were normalized to the average expression of β-*actin* ($n = 4$ separate bone marrow isolations, each performed in triplicate). *E*, representative images of the maximum intensity projection confocal images of cells incubated with DMSO or HC3 (250 μM) for 48 h and stained with DAPI or Nile Red. *Scale bars*, 10 μm. *Corner insets* are *enlarged* from the *yellow boxes*. Data are mean ± S.E. (*error bars*), where statistical significance for *A–C* is represented as follows: **, $p < 0.01$; ***, $p < 0.001$; ****, $p < 0.0001$ compared with control treatment as indicated, assessed by one-way ANOVA. Statistical significance for *D* is represented as follows: *, $p < 0.05$; **, $p < 0.01$ compared with DMSO control, determined by Student's *t* test.

inhibition was associated with an overall increase in macrophage PKC activity as assessed using a substrate motif antibody (Fig. 7), where in cells treated with the choline uptake inhibitor, an increased abundance of phosphorylated PKC substrates was observed.

Restoring PC levels but not inhibition of PKC rescues cytokine secretion

Inhibiting choline uptake directly skewed the macrophage inflammatory profile. As a final interrogation, we aimed to rescue the aberrant cytokine secretion via two independent approaches. We first supplemented macrophages with excess choline in the media (500 μM) in the presence of both HC3 and the CTL1-Ab. We hypothesized that excess choline would compete with the inhibitor and potentially restore choline uptake and metabolism. Interestingly, choline treatment rescued the levels of TNFα, IL-6, and IL-10 that were altered by HC3 (Fig. 8, *A–C*); however, in the presence of the CTL1-Ab, excess choline treatment was completely ineffective (Fig. 8, *D–F*). As a secondary approach, cells were treated with the conventional/novel PKC inhibitor bisindolylmaleimide I (BIM) (30) (20 μM) concurrently with HC3 and CTL1-Ab inhibition to potentially counter DAG-mediated PKC signaling. Independent of pharmacological or antibody-mediated choline inhibi-

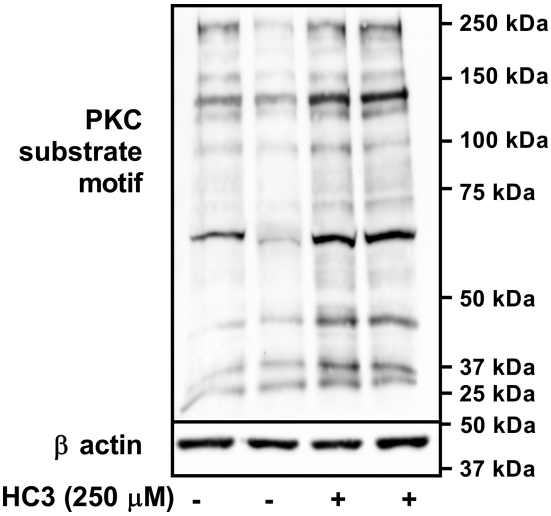

Figure 7. Inhibiting choline uptake is associated with higher PKC activity. Choline uptake was inhibited in BMDM for 48 h using HC3 (250 μM). Cell lysate was collected and immunoblotted using a PKC substrate motif antibody. Equal loading was confirmed by using β-actin, run on a duplicate gel ($n = 4$ separate isolations, each performed in duplicate). Blots are representative images of the biological replicates.

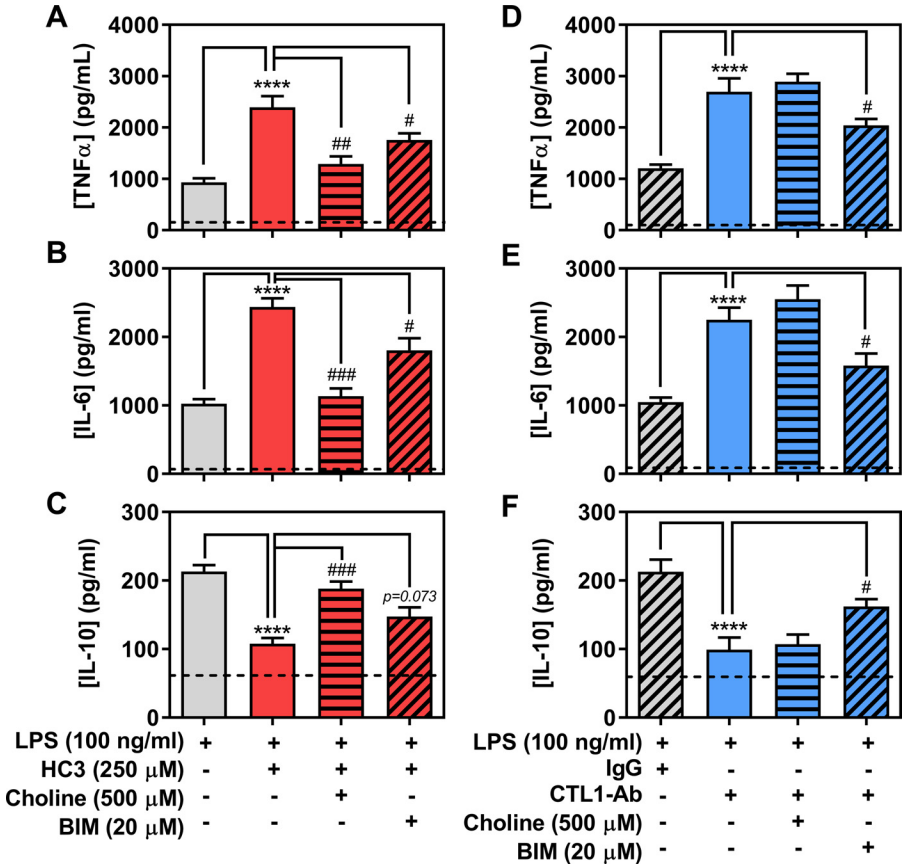

Figure 8. Extracellular choline or PKC inhibition rescues cytokine secretion profile. Cells were incubated in the presence or absence of HC3 (250 μM) or the CTL1-Ab (1:250) for 48 h and co-treated with excess choline chloride (500 μM) or the PKC inhibitor BIM (20 μM). The medium was removed, and cells were stimulated with 100 ng/ml LPS for 6 h, during which time the initial treatments were replenished. Secretion of TNFα (*A* and *D*), IL-6 (*B* and *E*), and IL-10 (C and *F*) into the medium was determined ($n = 5$ separate isolations, each performed in triplicate). Data are mean ± S.E. (*error bars*), where statistical significance is represented as follows: ****, $p < 0.0001$ compared with LPS-stimulated control or control IgG treatment; #, $p < 0.05$; ##, $p < 0.01$; ###, $p < 0.001$ compared with HC3, as indicated, assessed by one-way ANOVA.

tion, BIM treatment was partially able to correct the secreted levels of LPS-stimulated TNFα, IL-6, and IL-10 (Fig. 8, *A–F*). Finally, we confirmed that the supplementation of excess choline was able to dilute the effect of HC3-mediated inhibition on choline uptake and increased PC levels (Fig. 9*A*) but had no effect in cells treated with the CTL1-Ab. As expected, BIM treatment had no effect on PC levels (Fig. 9*B*).

Discussion

The metabolism of immune cells is intimately linked to cellular responses and programs (31, 32), but how phospholipid homeostasis is regulated in immunometabolism remains unclear. The current study looked to investigate the link between choline uptake, its subsequent metabolism, and inflammation in primary murine macrophages.

Macrophage activation is coupled with changes in membrane composition and dynamics; however, unlike other immune cells, such as T cell and natural killer cells, differentiated macrophages do not routinely undergo proliferative expansion. Hence, the induction of phospholipid biosynthesis, mainly PC, has been mainly attributed to a need for processes such as phagocytosis, organelle biogenesis, secretory functions, and endocytosis (33). Past work had established that acute LPS stimulation of elicited peritoneal macrophages increased the incorporation of [^{3}H]choline into PC; however, the mechanisms responsible have remained unclear (18). Here, we corroborate past findings and also show a higher rate of PC synthesis in response to LPS (Figs. 2 and 3). Coupled to this, we also demonstrate that the transport of choline via CTL1 is specifically up-regulated in LPS-stimulated macrophages (Figs. 1–3).

Augmented flux through the CDP-choline pathway has also been previously demonstrated in LPS-stimulated B cells (34), THP-1 monocytes (17), and elicited peritoneal macrophages (18, 19). Interestingly, in B cells, this was due to the up-regulation of choline phosphotransferase and lipin-1 genes, as well as an enhanced function of CCT, the rate-limiting enzyme in PC synthesis (34). A subsequent study by the same group using peritoneal macrophages revealed that LPS stimulation increased the gene expression of both the choline/ethanolamine phosphotransferase and CCT gene (*Pcyt1*). In our LPS-stimulated BMDM model, transcript expressions of genes in the CDP-choline pathway were unaltered (Fig. 3). However, it is possible that CCT function was augmented post-transcriptionally in response to higher levels of fatty acids (Fig. 2) and increased availability of intracellular choline (Fig. 1). Whereas previous studies did not investigate the expression of choline transporters in their model systems, there remains the potential that choline transport was also augmented to facilitate the

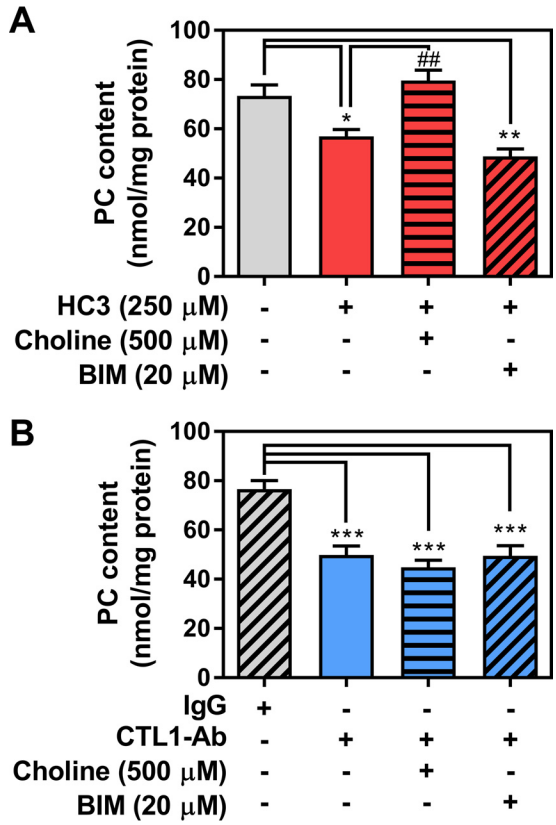

Figure 9. PC levels in the presence of choline or PKC inhibitor. *A*, cells were incubated with or without HC3 (250 μM), excess choline chloride (500 μM), or BIM (20 μM) for 48 h to assess PC levels ($n = 4$ separate isolations performed in duplicate). *B*, cells were treated with the CTL1-Ab (1:250), excess choline (500 μM), or BIM (20 μM) to assess PC levels ($n = 4$ separate isolations performed in duplicate). Data are mean ± S.E. (*error bars*), where statistical significance is represented as follows: *, $p < 0.05$; **, $p < 0.01$; ***, $p < 0.001$ compared with indicated control; ##, $p < 0.01$ compared with HC3 (*A*) group, as indicated, assessed by one-way ANOVA.

increased PC biosynthesis in LPS-stimulated B cells and peritoneal macrophages.

The increase in LPS-stimulated choline uptake was associated with higher levels of PC. However, coupled to this was an overall increase in *de novo* lipogenesis. Although it is well-known that LPS and other pro-inflammatory stimuli polarize macrophages toward a cellular program that favors glucose uptake, glycolysis, and diminished fatty acid β-oxidation (35, 36), it was recently shown that this augmented glucose metabolism is at least partly responsible for the higher levels of fatty acid synthesis and TG storage (25). Moreover, during monocyte-macrophage differentiation, sterol regulatory element–binding protein–induced fatty acid synthesis is also bolstered and directly facilitates increases in phospholipid synthesis (37). This presents a potential scenario whereby upon LPS stimulation, glucose uptake and transcriptional programs drive fatty acid and TG synthesis as well as choline uptake to facilitate PC synthesis. Whether diminishing the availability of choline or inhibiting choline uptake perturbs this LPS-derived increase in fatty acid production has yet to be investigated.

When human THP-1 monocytes underwent phorbol ester–induced differentiation into macrophages, this was accompanied by a similar disappearance of CTL1 from the cell surface and a presumed reduction in PC synthesis (although this was never measured) (5). In primary macrophages, we now demonstrate that the only choline transporters expressed are *Slc44a1* and *Slc44a2* (Fig. 3*A*) (data not shown). Moreover, LPS stimulation induces the transcript expression of both the CTL1 and CTL2 genes, while at the protein level, only CTL1 was increased (Fig. 3*B*). The mechanism by which only the CTL1 protein is up-regulated is unclear. However, in subsequent experiments, we used increasing amounts of a CTL1-specific antibody to show that the majority of macrophage choline uptake was CTL1-dependent, as PC synthesis decreased more than 80% and cell viability was compromised as antibody concentrations increased (Fig. 4) (data not shown). A previous characterization of the CTL1 promoter uncovered a putative binding site for the NF-κB transcription factor, which was validated *in vitro* by gel mobility shift assays (38). Future studies are needed to verify whether NF-κB signaling is required for the LPS-induced up-regulation of CTL1 and hence choline uptake.

Whereas LPS stimulation of macrophages increases choline uptake and metabolism, we next aimed to ask the reciprocal question as to the importance of choline uptake and metabolism for macrophage inflammation (in response to LPS). We initially hypothesized that choline uptake and subsequent incorporation into PC in the macrophage would be important to accommodate the increased burden of cytokine secretion and trafficking, which involve the ER and *trans*-Golgi network (39, 40). The Chinese hamster ovary cell line MT58 (containing a thermosensitive mutation in the *Pcyt1* gene) has provided an excellent model to study PC depletion and has shown that reductions of PC levels lead to ER and Golgi dysfunction (41–43). Similar defects in protein trafficking were observed in peritoneal macrophages derived from CCTα-deficient mice, where reduced PC synthesis was accompanied by intracellular aggregation and reduced secretion of TNF and IL-6 (19).

Contrary to our hypothesis, when we inhibited choline uptake with HC3 or with a CTL1-specific antibody for a period of 48 h followed by a 6-h stimulation with LPS, the secretion of inflammatory cytokines, such as TNFα and IL-6, was higher, whereas IL-10 secretion was lower (Fig. 5). Interestingly, HC3 or CTL1-Ab treatment effectively inhibited choline uptake and diminished PC levels in the cell (Fig. 4); however, no defects in cytokine secretion were observed. There remains the potential that experimental differences could be the root of the divergent phenotype between our model of choline depletion and the CCTα-deficient macrophages. First, we used primary BMDM, whereas thioglycollate was used to elicit peritoneal macrophages from WT and CCTα-deficient mice (19). It is well-established that the phenotypic and metabolic differences between these two primary macrophage populations are many; therefore, it is unlikely that a direct comparison can be made (44). Moreover, we inhibited choline uptake, both pharmacologically and using antibody treatments for 48 h. This is compared with a genetic knockout, in which compensatory mechanisms (apparent or not) may have been at play. Interestingly, previous studies have shown an anti-inflammatory role for exogenous choline in primary macrophages from α7 nicotinic acetylcholine receptor null mice, whereby in these cells, TNFα release was blunted (45). Moreover, PC supplementation stemmed pro-inflammatory programming of intestinal epithe-

lial cells (46). Taken together, these findings suggest that choline and PC supplementation may have anti-inflammatory implications that are both independent of the cholinergic system and extend beyond innate immune cells.

In our model, following the chronic inhibition of choline uptake, LPS-triggered TNFα and IL-6 were higher, whereas IL-10 secretion was lower, which is potentially indicative of a pro-inflammatory shift. Past work has demonstrated that choline deficiency can induce phospholipase C activity to lower sphingomyelin and increase ceramide levels (47), which has ties to apoptotic and pro-inflammatory signaling (48). In addition to providing the major membrane phospholipid component, PC is also considered an important reservoir for AA-derived lipid messengers, such as prostaglandins and leukotrienes (20, 21, 49). Future studies could test the potential that the inhibition of PC synthesis alters downstream AA-derived signaling pathways to differentially affect cytokine release.

Phospholipid metabolism is intricately linked to FA and lipid homeostasis. There have been many examples in various cellular systems whereby the disruption of either the CDP-choline or CDP-ethanolamine pathways, which produce PC and phosphatidylethanolamine, respectively, have resulted in a redirection of DAG and aberrant lipid homeostasis (19, 47, 50–52). In our studies, choline deficiency induced by pharmacological or CTL1-specific inhibition limited the availability of the initial substrate in PC biosynthesis and hence led to 1) a reduced flux through the CDP-choline pathway and 2) an accumulation of DAG and TG. Although the cellular consequence of increased TG remains unclear, HC3-treated cells had higher expression of *Dgat2* and more defined lipid droplet formation, which is in keeping with a redirection of DAG toward TG. However, how TG metabolism may be altered under this condition warrants further investigation. We provide evidence for an up-regulation of PKC activation that was associated with higher DAG levels. Previous work in macrophages has demonstrated that DAG-mediated PKC activation can increase signal transduction through the NF-κB pathway, and treatment of macrophages with a PKC inhibitor reduces LPS-induced inflammatory signaling (27–29). Inhibition of PKC activity with BIM was partially effective at restoring normal cytokine secretion in our study, where TNFα and IL-6 were lower and IL-10 was higher (Fig. 8). Although this points to the involvement of PKC signaling, 1) an exhaustive panel of isoform inhibitors was not used, and 2) at the concentration used (20 μM), the specificity for conventional and novel PKC isoforms is reduced. Although pharmacological inhibition and antibody occlusion provide models of choline deficiency, it would be interesting to interrogate the role of CTL1-mediated choline uptake in primary macrophages from CTL1-deficient mice; however, to date, no mouse model has been described.

We demonstrate that pro-inflammatory polarization increased choline uptake and subsequently PC biosynthesis, which primes the macrophages to respond appropriately to immune stimuli (Fig. S6). Augmented choline uptake is probably CTL1-dependent and would provide necessary amounts of PC to membranes (organelle and plasma membranes) for the packaging and secretion of cytokines. Moreover, we show that modulating PC biosynthesis has the capacity to reprogram immune responsiveness in primary macrophages and highlights a reciprocal link between choline metabolism and macrophage inflammation.

Experimental procedures

Animals

Mice (C57Bl/6J) were originally purchased from Jackson Laboratories (stock no. 00064) and bred in a pathogen-free facility in the University of Ottawa animal facility. Mice were maintained on a 12-h light/dark cycle (lights on at 7:00 a.m.) and housed at 23 °C with bedding enrichment. Male and female mice ages 8–16 weeks were used for the generation of primary macrophages as described below. All animal procedures were approved by the University of Ottawa Animal Care Committee.

Isolation, culturing, and polarization of bone marrow macrophages

BMDM were isolated and cultured as described previously (53, 54). Bone marrow cells were obtained from the femur and tibia by centrifugation. Briefly, mice were euthanized, and the bones were dissected free of all musculature and connective tissue. Bones from each leg were cut and placed inside a 0.5-ml tube with a hole punctured in the bottom by an 18-gauge needle, which was placed inside a larger 1.5-ml tube. To the 0.5 ml (bone-containing tube), 100 μl of DMEM was added, and cells were obtained by centrifugation at 4000 rpm. Bone marrow cells were resuspended in 1 ml of DMEM and filtered through a 40-μm filter to remove any debris and made up in a final volume of 85 ml of complete DMEM (4.5 g/liter glucose, with 1× L-glutamine and sodium pyruvate (Wisent)), supplemented with 10% FBS (Wisent) and 1% penicillin/streptomycin (Fisher). Cells were differentiated into macrophages using 15% L929-conditioned medium as a source of macrophage colony–stimulating factor. Cells were plated into 10- or 15-cm dishes and allowed to differentiate for 7 days. On day 8, cells were lifted by gentle cell scraping, counted, and seeded into culture plates for experiments (2.5×10^5 for 24-well plates, 4×10^5 for 12-well plates, and 1×10^6 for 6-well plates). Cells were treated for 48 h with or without 100 ng/ml LPS (*Escherichia coli* B4, Sigma-Aldrich) to skew BMDM toward an LPS-polarized phenotype.

Choline uptake experiments

The rate of choline uptake was determined by measuring [^{3}H]choline chloride (PerkinElmer Life Sciences) uptake over time. Cells were seeded into 24-well plates. One hour before uptake, medium was removed, and cells were washed with PBS before being incubated in Krebs-Ringer-HEPES buffer (KRH; 130 mM NaCl, 1.3 mM KCl, 2.2 mM $CaCl_2$, 1.2 mM $MgSO_4$, 1.2 mM KH_2PO_4, 10 mM HEPES, pH 7.4, and 10 mM glucose) to remove exogenous choline for 1 h. Immediately before uptake, cells were washed again, followed by the addition of KRH containing 1 μCi/ml [^{3}H]choline, and were incubated at 37 °C for the desired time (1–30 min). Following incubation, cells were washed twice with ice-cold KRH buffer and lysed in 150 μl of 0.1 M NaOH, and an aliquot was used to determine radioactivity by liquid scintillation counting. Total cellular protein was

determined using a BCA protein assay (Thermo Fisher Scientific) according to the manufacturer's instructions. Choline uptake was expressed as pmol of choline/mg of protein. Choline transport kinetics and uptake inhibition to the choline analogue HC3 were performed as we have described previously (5).

[^{3}H]Choline, [^{3}H]acetate, and [^{3}H]glycerol incorporation into lipids

Macrophages were seeded into 6-well plates. Cells were washed with PBS and treated with DMEM containing 1 μCi/ml [^{3}H]choline, [^{3}H]acetate, or [^{3}H]glycerol for the indicated time (2–48 h). Cells were then washed twice with PBS and lysed with a freeze/thaw cycle at −80 °C in 200 μl of PBS. Lipids were extracted using the method of Bligh and Dyer (55), and the chloroform (lipid-containing) phase was evaporated to dryness under nitrogen gas and resuspended in 50 μl of chloroform. Phospholipid and neutral lipids were separated using TLC as described previously (51), and the radioactivity associated with each lipid was measured using liquid scintillation counting. Total protein was measured by a BCA assay.

PC degradation

For pulse-chase experiments to determine PC degradation, macrophages were seeded into 12-well plates and pulsed for 2 h with 1 μCi/ml [^{3}H]choline-containing DMEM. Radiolabeled medium was then removed, and the cells were washed with PBS and chased with DMEM containing an excess (500 μM) of unlabeled choline for 1, 2, and 4 h. For analyses, the cells were washed twice with ice-cold PBS and processed as described above.

Chronic choline uptake inhibition and determination of PC content

Choline uptake was chronically inhibited by incubating BMDM with a 250 μM concentration of the high/intermediate-affinity choline transport inhibitor HC3 for 48 h. To specifically test the role of CTL1, cells were incubated for 48 h in the presence of either a CTL1-specific antibody (a gift from Dr. Marica Bakovic, University of Guelph) or an IgG isotype control (Jackson ImmunoResearch), both at a 1:250 dilution. In parallel experiments, macrophages were treated with HC3 and CTL1 antibody in the presence of 500 μM choline chloride (Sigma) or 20 μM BIM (a gift from Dr. Marceline Côté; originally purchased from Cayman Chemical). To determine PC content, cells were plated in 6-well plates and treated as described above. Following 48-h treatment, cells were washed with ice-cold PBS and processed using a PC assay kit (Abcam) as per the manufacturer's instructions. Duplicate wells were used for protein determination, and PC content was expressed as nmol/mg protein.

Determination of cytokine secretion

Cells were plated in 24-well plates. Following chronic (48 h) choline uptake inhibition, as described above, BMDM were stimulated with or without 100 ng/ml LPS for 6 h in 300 μl of medium (HC3 or CTL1-Ab was replenished during this treatment). The medium was collected and stored at −80 °C. Cytokines were determined initially using the Mouse Cytokine Array Panel A (R&D Systems), according to the manufacturer's instructions. For TNFα, IL-6, IL-10, and IL-1β, Duoset ELISA kits (R&D Systems) were used, again in accordance with the manufacturer's instructions.

Transcript expression

Total RNA was isolated from BMDM using the TriPure reagent protocol (Roche Applied Science). Isolated RNA was resuspended in 30 μl of RNase/DNase-free water (Wisent). The QuantiNova^{TM} reverse transcription kit (Qiagen) was used to synthesize cDNA according to kit instructions. To determine transcript expression, the QuantiNova^{TM} probe PCR kit (Qiagen) was used in combination with TaqMan primer–probe sets. qPCRs were run on the Roto-Gene Q (Qiagen). Relative transcript expression was determined using the $\Delta\Delta Ct$ method and normalized to the average expression of β-*actin* and *Tbp* (56).

Immunoblotting

Following treatments, BMDM were washed twice with PBS and lysed in a denaturing lysis buffer (50 mM Tris-HCl, pH 7.5, 150 mM NaCl, 1 mM EDTA, 0.5% Triton X-100, 0.5% Nonidet P-40, 100 μM sodium orthovanadate, and protease inhibitor mixture tablet; Roche Applied Science), or for CTL1 immunoblotting, a nondenaturing native lysis buffer (identical to denaturing lysis buffer but lacking Triton X-100 and Nonidet P-40) was used. Proteins were equally loaded onto an 8% SDS-polyacrylamide gel, where samples being probed for CTL1 were not boiled before loading. We have found that although previous literature documents that full nondenaturing conditions are optimal for identifying a single CTL1 (~72 kDa) band via immunoblotting (6), a combination of native lysis buffer and denaturing SDS-PAGE is ideal for cultured macrophages. Gels were transferred onto a polyvinylidene difluoride membrane (17 min at 1.3 A) using the Trans-Blot® Turbo^{TM} transfer system (Bio-Rad) with Bjerrum Schafer-Nielsen buffer (48 mM Tris, 39 mM glycine, 20% methanol). Membranes were blocked for 1 h in 5% BSA and then incubated at 4 °C overnight in CTL1, CTL2 (Abcam, catalog no. 177877), PKC substrate motif (CST, catalog no. 6967), or β-actin rabbit (horseradish peroxidase–conjugated, CST, catalog no. 5125). A 1:1000 dilution of stock antibodies in 5% BSA was used for primary antibody incubations. The following day, membranes were washed four times in TBS-T (20 mM Tris, 150 mM NaCl, 0.05% Tween® 20), and all blots except β-actin were incubated for 1 h in HRP-conjugated anti-rabbit IgG (CST, catalog no. 7074, 1:5000 dilution). Clarity^{TM} Western ECL solution (Bio-Rad) was applied to membranes, which were visualized using the LAS 4010 ImageQuant imaging system (General Electric). Densitometry analysis was performed using ImageJ software (version 1.48), where CTL1 and CTL2 expressions were normalized to β-actin.

HPLC-ESI-MS/MS lipidomics

Macrophages were treated as described above and extracted using a modified Bligh and Dyer protocol (55) described previously (57–59). Briefly, cells were collected, counted, washed with PBS, and pelleted at a concentration of 1×10^6 cells/sample. PBS was removed, and pellets were stored at −80 °C until extraction. Four milliliters of acidified methanol (Fisher, cata-

log no. BP1105-4) containing 2% acetic acid (Fisher, catalog no. A38-212) were added to cell pellets and transferred using a glass Pasteur pipette into Kimble 10-ml glass threaded tubes (disposable; VWR, catalog no. 21020-640). MS grade lipid standards, PC(13:0/0:0) (90.7 ng; Avanti, LM-1600) and PC(12:0/13:0) (100 ng; Avanti, LM-1000), were added to the homogenate at the time of extraction. Chloroform (Fisher, catalog no. C298-500) and 0.1 M sodium acetate (J.T. Baker, catalog no. 9831-03) were added to each sample at a final ratio of acidified methanol/chloroform/sodium acetate (2:1.9:1.6). Samples were vortexed and centrifuged at 600 × *g* for 5 min at 4 °C. The organic phase was retained, and the aqueous phase was successively back-extracted using chloroform three times. The four organic extracts were combined and evaporated at room temperature under a constant stream of nitrogen gas. Final extracts were solubilized in 300 μl of anhydrous ethanol (Commercial Alcohols, P016EAAN), flushed with nitrogen gas, and stored at −80 °C in amber glass vials (Chromatographic Specialties, C779100AW).

Lipid samples were analyzed using a triple quadrupole-linear ion trap mass spectrometer QTRAP 5500 equipped with a Turbo V ion source (AB SCIEX, Concord, Canada). Samples were prepared for HPLC injection by mixing 5 μl of lipid extract with 5 μl of an internal standard mixture consisting of PC(O-16:0-d_4/0:0) (2.5 ng; Cayman, 360906), PC(O-18:0-d_4/0:0) (2.5 ng; Cayman, 10010228), PC(O-16:0-d_4/2:0) (1.25 ng; Cayman, 360900), PC(O-18:0-d_4/2:0) (1.25 ng; Cayman, 10010229), PC(15:0/18:1-d_7) (1.25 ng; Avanti Polar Lipids, 791637C), PC(18:1-d_7/0:0) (1.25 ng; Avanti Polar Lipids, 791643C), SM(d18:1/18:1-d_9) (1.25 ng; Avanti Polar Lipids, 791649C) in EtOH and 13.5 μl of solvent A (see below). HPLC was performed with an Agilent Infinity II system operating at a flow rate of 10 μl/min with 3-μl sample injections by an autosampler maintained at 4 °C. A 100 mm × 250-μm (inner diameter) capillary column packed with ReproSil-Pur 200 C18 (particle size of 3 μm and pore size of 200 Å, Dr. A. Maisch, Ammerbruch, Germany) was used with a binary solvent gradient consisting of water with 0.1% formic acid (Fluka, catalog no. 56302) and 10 mM ammonium acetate (OmniPur, catalog no. 2145) (solvent A) and ACN/IPA (J.T. Baker, catalog no. 9829-03; Fisher, catalog no. A416-4) (5:2; v/v) with 0.1% formic acid and 10 mM ammonium acetate (solvent B). The gradient started from 30% B, reached 100% B in 8 min, and maintained for 37 min. The solvent composition returned to 30% B within 1 min and maintained for 14 min to re-equilibrate the column before the next sample injection. The PC and SM lipidome was first profiled using a precursor ion scan in positive ion mode monitoring transitions from protonated molecular ions to *m*/*z* 184.1. Data acquisition for quantification was then performed in the positive ion mode using selected reaction monitoring (SRM), monitoring transitions from protonated molecular ions to *m*/*z* 184.1. Molecular identities were confirmed in a single HPLC-SRM information-dependent acquisition (IDA)-enhanced product ion (EPI) experiment in which SRM was used as a survey scan to identify target analytes, and an IDA of EPI spectra was acquired in the linear ion trap. After acquisition, the EPI spectra were examined for structural determination. Instrument control and data acquisition were performed with Analyst software version 1.6.2 (AB SCIEX). MultiQuant 3.0.2 software version 3.0.8664.0 (SCIEX) was used for processing of quantitative multiple-reaction monitoring data. For quantification, raw peak areas were corrected for extraction efficiency and instrument response by normalization to internal standards added at the time of extraction. Lipid abundances were then expressed as pmol equivalents of the internal standard PC(13:0/0:0) per 1 × 10^6 cells.

Flow cytometry

Macrophages were plated in 6-well plates and treated with DMSO or HC3 (250 μM) for 48 h. After washing with PBS, cells were scraped and stained with Zombie Aqua dye (BioLegend) for 30 min on ice. Cells were washed and resuspended in DAPI-containing FACS buffer (1% BSA, 2 mM EDTA in PBS) and acquired using a FACSCelesta flow cytometer (BD Biosciences). Viability and cell size were calculated from the frequency of live cells among singlet cell events and forward scatter, respectively.

Confocal microscopy

Macrophages were plated in 24-well plates containing #1.5 glass coverslips and treated with DMSO or HC3 (250 μM) for 48 h. After washing with PBS, coverslips were fixed with 1% paraformaldehyde for 15 min at RT and permeabilized with 0.1% Triton X-100 in PBS for 5 min at RT. Cells were stained with DAPI and Nile Red for 15 min at RT and mounted using Prolong Antifade Gold (Thermo Fisher) on SuperFrost Plus slides (Thermo Fisher). *Z*-stack images were acquired using an LSM800 AxioObserverZ1 microscope (Zeiss) with a ×63 (1.4 numerical aperture) oil objective. Images were equally adjusted and using FIJI software (National Institutes of Health).

Statistics

All statistical analyses were performed using Prism version 7 (GraphPad Software Inc.). Transcript and protein expression were compared using a nonpaired Student's *t* test. Choline incorporation data were analyzed using a two-way ANOVA. Kinetic curves, HC3 IC_{50} curve, and values were generated using the Prism version 7 nonlinear regression Michaelis–Menten curve fit and nonlinear regression *versus* response with variable slopes curve fit, respectively. Chronic choline inhibition experiments and cytokine secretion experiments were analyzed using a one-way or two-way ANOVA as indicated, where significant difference between groups was determined by Tukey's *post hoc* test. For all comparisons, a *p* value of <0.05 was considered significant. Quantification of PC and sphingomyelin abundances was analyzed by two-way ANOVA with Holm–Sidak post hoc test. For all comparisons, a *p* value of <0.05 was considered significant.

Author contributions—S. A. S., K. D. M., and M. D. F. planned the experiments. S. A. S., K. D. M., N. D. L., P. G., J. R. C. N., and C. O. D. conducted the experiments and analyzed the results. T. N., H. X., and S. A. L. B. performed and analyzed lipidomic experiments. S. A. S., K. D. M., and M. D. F. wrote the manuscript, and all authors had a part in editing the manuscript.

Acknowledgments—We thank Dr. Marica Bakovic (University of Guelph) for kindly contributing the CTL1 antibody. We also thank Dr. Subash Sad, Dr. Marceline Côté, Corina Warkentin, Graham Gould Maule, and Tyler Smith for helpful discussions and reagents.

References

1. Kawasaki, T., and Kawai, T. (2014) Toll-like receptor signaling pathways. *Front. Immunol.* **5,** 461 Medline
2. Bianchi, M. E. (2007) DAMPs, PAMPs and alarmins: all we need to know about danger. *J. Leukoc. Biol.* **81,** 1–5 CrossRef Medline
3. Kennedy, E. P., and Weiss, S. B. (1956) The function of cytidine coenzymes in the biosynthesis of phospholipides. *J. Biol. Chem.* **222,** 193–214 Medline
4. Cornell, R. B., and Ridgway, N. D. (2015) CTP:phosphocholine cytidylyltransferase: function, regulation, and structure of an amphitropic enzyme required for membrane biogenesis. *Prog. Lipid Res.* **59,** 147–171 CrossRef Medline
5. Fullerton, M. D., Wagner, L., Yuan, Z., and Bakovic, M. (2006) Impaired trafficking of choline transporter-like protein-1 at plasma membrane and inhibition of choline transport in THP-1 monocyte-derived macrophages. *Am. J. Physiol. Cell Physiol.* **290,** C1230–C1238 CrossRef Medline
6. Michel, V., and Bakovic, M. (2009) The solute carrier 44A1 is a mitochondrial protein and mediates choline transport. *FASEB J.* **23,** 2749–2758 CrossRef Medline
7. da Costa, K. A., Corbin, K. D., Niculescu, M. D., Galanko, J. A., and Zeisel, S. H. (2014) Identification of new genetic polymorphisms that alter the dietary requirement for choline and vary in their distribution across ethnic and racial groups. *FASEB J.* **28,** 2970–2978 CrossRef Medline
8. Haga, T. (2014) Molecular properties of the high-affinity choline transporter CHT1. *J. Biochem.* **156,** 181–194 CrossRef Medline
9. Okuda, T., Haga, T., Kanai, Y., Endou, H., Ishihara, T., and Katsura, I. (2000) Identification and characterization of the high-affinity choline transporter. *Nat. Neurosci.* **3,** 120–125 CrossRef Medline
10. Gorboulev, V., Ulzheimer, J. C., Akhoundova, A., Ulzheimer-Teuber, I., Karbach, U., Quester, S., Baumann, C., Lang, F., Busch, A. E., and Koepsell, H. (1997) Cloning and characterization of two human polyspecific organic cation transporters. *DNA Cell Biol.* **16,** 871–881 CrossRef Medline
11. Sweet, D. H., Miller, D. S., and Pritchard, J. B. (2001) Ventricular choline transport: a role for organic cation transporter 2 expressed in choroid plexus. *J. Biol. Chem.* **276,** 41611–41619 CrossRef Medline
12. Traiffort, E., O'Regan, S., and Ruat, M. (2013) The choline transporter-like family SLC44: properties and roles in human diseases. *Mol. Aspects Med.* **34,** 646–654 CrossRef Medline
13. Fujita, T., Shimada, A., Okada, N., and Yamamoto, A. (2006) Functional characterization of Na^+-independent choline transport in primary cultures of neurons from mouse cerebral cortex. *Neurosci. Lett.* **393,** 216–221 CrossRef Medline
14. Inazu, M., Takeda, H., and Matsumiya, T. (2005) Molecular and functional characterization of an Na^+-independent choline transporter in rat astrocytes. *J. Neurochem.* **94,** 1427–1437 CrossRef Medline
15. Ishiguro, N., Oyabu, M., Sato, T., Maeda, T., Minami, H., and Tamai, I. (2008) Decreased biosynthesis of lung surfactant constituent phosphatidylcholine due to inhibition of choline transporter by gefitinib in lung alveolar cells. *Pharm. Res.* **25,** 417–427 CrossRef Medline
16. Wille, S., Szekeres, A., Majdic, O., Prager, E., Staffler, G., Stöckl, J., Kunthalert, D., Prieschl, E. E., Baumruker, T., Burtscher, H., Zlabinger, G. J., Knapp, W., and Stockinger, H. (2001) Characterization of CDw92 as a member of the choline transporter-like protein family regulated specifically on dendritic cells. *J. Immunol.* **167,** 5795–5804 CrossRef Medline
17. Chu, A. J. (1992) Bacterial lipopolysaccharide stimulates phospholipid synthesis and phosphatidylcholine breakdown in cultured human leukemia monocytic THP-1 cells. *Int. J. Biochem.* **24,** 317–323 CrossRef Medline
18. Grove, R. I., Allegretto, N. J., Kiener, P. A., and Warr, G. A. (1990) Lipopolysaccharide (LPS) alters phosphatidylcholine metabolism in elicited peritoneal macrophages. *J. Leukoc. Biol.* **48,** 38–42 CrossRef Medline
19. Tian, Y., Pate, C., Andreolotti, A., Wang, L., Tuomanen, E., Boyd, K., Claro, E., and Jackowski, S. (2008) Cytokine secretion requires phosphatidylcholine synthesis. *J. Cell Biol.* **181,** 945–957 CrossRef Medline
20. Lennartz, M. R. (1999) Phospholipases and phagocytosis: the role of phospholipid-derived second messengers in phagocytosis. *Int. J. Biochem. Cell Biol.* **31,** 415–430 CrossRef Medline
21. Balsinde, J., Balboa, M. A., and Dennis, E. A. (1997) Inflammatory activation of arachidonic acid signaling in murine P388D1 macrophages via sphingomyelin synthesis. *J. Biol. Chem.* **272,** 20373–20377 CrossRef Medline
22. Zhang, C., Wang, Y., Wang, F., Wang, Z., Lu, Y., Xu, Y., Wang, K., Shen, H., Yang, P., Li, S., Qin, X., and Yu, H. (2017) Quantitative profiling of glycerophospholipids during mouse and human macrophage differentiation using targeted mass spectrometry. *Sci. Rep.* **7,** 412 CrossRef Medline
23. Im, S. S., Yousef, L., Blaschitz, C., Liu, J. Z., Edwards, R. A., Young, S. G., Raffatellu, M., and Osborne, T. F. (2011) Linking lipid metabolism to the innate immune response in macrophages through sterol regulatory element binding protein-1a. *Cell Metab.* **13,** 540–549 CrossRef Medline
24. Huang, Y. L., Morales-Rosado, J., Ray, J., Myers, T. G., Kho, T., Lu, M., and Munford, R. S. (2014) Toll-like receptor agonists promote prolonged triglyceride storage in macrophages. *J. Biol. Chem.* **289,** 3001–3012 CrossRef Medline
25. Feingold, K. R., Shigenaga, J. K., Kazemi, M. R., McDonald, C. M., Patzek, S. M., Cross, A. S., Moser, A., and Grunfeld, C. (2012) Mechanisms of triglyceride accumulation in activated macrophages. *J. Leukoc. Biol.* **92,** 829–839 CrossRef Medline
26. Zeisel, S. H., Da Costa, K. A., Franklin, P. D., Alexander, E. A., Lamont, J. T., Sheard, N. F., and Beiser, A. (1991) Choline, an essential nutrient for humans. *FASEB J.* **5,** 2093–2098 CrossRef Medline
27. Zhou, X., Yang, W., and Li, J. (2006) Ca^{2+}- and protein kinase C-dependent signaling pathway for nuclear factor-κB activation, inducible nitric-oxide synthase expression, and tumor necrosis factor-α production in lipopolysaccharide-stimulated rat peritoneal macrophages. *J. Biol. Chem.* **281,** 31337–31347 CrossRef Medline
28. Asehnoune, K., Strassheim, D., Mitra, S., Yeol Kim, J., and Abraham, E. (2005) Involvement of PKCα/β in TLR4 and TLR2 dependent activation of NF-κB. *Cell. Signal.* **17,** 385–394 CrossRef Medline
29. Foey, A. D., and Brennan, F. M. (2004) Conventional protein kinase C and atypical protein kinase Cζ differentially regulate macrophage production of tumour necrosis factor-α and interleukin-10. *Immunology* **112,** 44–53 CrossRef Medline
30. Toullec, D., Pianetti, P., Coste, H., Bellevergue, P., Grand-Perret, T., Ajakane, M., Baudet, V., Boissin, P., Boursier, E., and Loriolle, F. (1991) The bisindolylmaleimide GF 109203X is a potent and selective inhibitor of protein kinase C. *J. Biol. Chem.* **266,** 15771–15781 Medline
31. Peyssonnaux, C., Datta, V., Cramer, T., Doedens, A., Theodorakis, E. A., Gallo, R. L., Hurtado-Ziola, N., Nizet, V., and Johnson, R. S. (2005) HIF-1α expression regulates the bactericidal capacity of phagocytes. *J. Clin. Invest.* **115,** 1806–1815 CrossRef Medline
32. Galván-Peña, S., and O'Neill, L. A. (2014) Metabolic reprograming in macrophage polarization. *Front. Immunol.* **5,** 420 Medline
33. Ecker, J., Liebisch, G., Englmaier, M., Grandl, M., Robenek, H., and Schmitz, G. (2010) Induction of fatty acid synthesis is a key requirement for phagocytic differentiation of human monocytes. *Proc. Natl. Acad. Sci. U.S.A.* **107,** 7817–7822 CrossRef Medline
34. Fagone, P., Sriburi, R., Ward-Chapman, C., Frank, M., Wang, J., Gunter, C., Brewer, J. W., and Jackowski, S. (2007) Phospholipid biosynthesis program underlying membrane expansion during B-lymphocyte differentiation. *J. Biol. Chem.* **282,** 7591–7605 CrossRef Medline
35. Norata, G. D., Caligiuri, G., Chavakis, T., Matarese, G., Netea, M. G., Nicoletti, A., O'Neill, L. A., and Marelli-Berg, F. M. (2015) The cellular and molecular basis of translational immunometabolism. *Immunity* **43,** 421–434 CrossRef Medline
36. Langston, P. K., Shibata, M., and Horng, T. (2017) Metabolism supports macrophage activation. *Front. Immunol.* **8,** 61 Medline
37. Gordon, S., Plüddemann, A., and Martinez Estrada, F. (2014) Macrophage heterogeneity in tissues: phenotypic diversity and functions. *Immunol. Rev.* **262,** 36–55 CrossRef Medline

38. Yuan, Z., Tie, A., Tarnopolsky, M., and Bakovic, M. (2006) Genomic organization, promoter activity, and expression of the human choline transporter-like protein 1. *Physiol. Genomics* **26,** 76–90 CrossRef Medline
39. Manderson, A. P., Kay, J. G., Hammond, L. A., Brown, D. L., and Stow, J. L. (2007) Subcompartments of the macrophage recycling endosome direct the differential secretion of IL-6 and TNFα. *J. Cell Biol.* **178,** 57–69 CrossRef Medline
40. Murray, R. Z., and Stow, J. L. (2014) Cytokine secretion in macrophages: SNAREs, Rabs, and membrane trafficking. *Front. Immunol.* **5,** 538 Medline
41. Marciniak, S. J., Yun, C. Y., Oyadomari, S., Novoa, I., Zhang, Y., Jungreis, R., Nagata, K., Harding, H. P., and Ron, D. (2004) CHOP induces death by promoting protein synthesis and oxidation in the stressed endoplasmic reticulum. *Genes Dev.* **18,** 3066–3077 CrossRef Medline
42. Nishitoh, H. (2012) CHOP is a multifunctional transcription factor in the ER stress response. *J. Biochem.* **151,** 217–219 CrossRef Medline
43. van der Sanden, M. H., Houweling, M., van Golde, L. M., and Vaandrager, A. B. (2003) Inhibition of phosphatidylcholine synthesis induces expression of the endoplasmic reticulum stress and apoptosis-related protein CCAAT/enhancer-binding protein-homologous protein (CHOP/GADD153). *Biochem. J.* **369,** 643–650 CrossRef Medline
44. Artyomov, M. N., Sergushichev, A., and Schilling, J. D. (2016) Integrating immunometabolism and macrophage diversity. *Semin. Immunol.* **28,** 417–424 CrossRef Medline
45. Rowley, T. J., McKinstry, A., Greenidge, E., Smith, W., and Flood, P. (2010) Antinociceptive and anti-inflammatory effects of choline in a mouse model of postoperative pain. *Br. J. Anaesth.* **105,** 201–207 CrossRef Medline
46. Treede, I., Braun, A., Sparla, R., Kühnel, M., Giese, T., Turner, J. R., Anes, E., Kulaksiz, H., Füllekrug, J., Stremmel, W., Griffiths, G., and Ehehalt, R. (2007) Anti-inflammatory effects of phosphatidylcholine. *J. Biol. Chem.* **282,** 27155–27164 CrossRef Medline
47. Yen, C. L., Mar, M. H., and Zeisel, S. H. (1999) Choline deficiency-induced apoptosis in PC12 cells is associated with diminished membrane phosphatidylcholine and sphingomyelin, accumulation of ceramide and diacylglycerol, and activation of a caspase. *FASEB J.* **13,** 135–142 CrossRef Medline
48. Schütze, S., Potthoff, K., Machleidt, T., Berkovic, D., Wiegmann, K., and Krönke, M. (1992) TNF activates NF-kappa B by phosphatidylcholine-specific phospholipase C-induced "acidic" sphingomyelin breakdown. *Cell* **71,** 765–776 CrossRef Medline
49. Dennis, E. A., and Norris, P. C. (2015) Eicosanoid storm in infection and inflammation. *Nat. Rev. Immunol.* **15,** 511–523 CrossRef Medline
50. Selathurai, A., Kowalski, G. M., Burch, M. L., Sepulveda, P., Risis, S., Lee-Young, R. S., Lamon, S., Meikle, P. J., Genders, A. J., McGee, S. L., Watt, M. J., Russell, A. P., Frank, M., Jackowski, S., Febbraio, M. A., and Bruce, C. R. (2015) The CDP-ethanolamine pathway regulates skeletal muscle diacylglycerol content and mitochondrial biogenesis without altering insulin sensitivity. *Cell Metab.* **21,** 718–730 CrossRef Medline
51. Fullerton, M. D., Hakimuddin, F., Bonen, A., and Bakovic, M. (2009) The development of a metabolic disease phenotype in CTP:phosphoethanolamine cytidylyltransferase-deficient mice. *J. Biol. Chem.* **284,** 25704–25713 CrossRef Medline
52. Leonardi, R., Frank, M. W., Jackson, P. D., Rock, C. O., and Jackowski, S. (2009) Elimination of the CDP-ethanolamine pathway disrupts hepatic lipid homeostasis. *J. Biol. Chem.* **284,** 27077–27089 CrossRef Medline
53. Fullerton, M. D., Ford, R. J., McGregor, C. P., LeBlond, N. D., Snider, S. A., Stypa, S. A., Day, E. A., Lhoták, Š., Schertzer, J. D., Austin, R. C., Kemp, B. E., and Steinberg, G. R. (2015) Salicylate improves macrophage cholesterol homeostasis via activation of Ampk. *J. Lipid Res.* **56,** 1025–1033 CrossRef Medline
54. Galic, S., Fullerton, M. D., Schertzer, J. D., Sikkema, S., Marcinko, K., Walkley, C. R., Izon, D., Honeyman, J., Chen, Z. P., van Denderen, B. J., Kemp, B. E., and Steinberg, G. R. (2011) Hematopoietic AMPK β1 reduces mouse adipose tissue macrophage inflammation and insulin resistance in obesity. *J. Clin. Invest.* **121,** 4903–4915 CrossRef Medline
55. Bligh, E. G., and Dyer, W. J. (1959) A rapid method of total lipid extraction and purification. *Can. J. Biochem. Physiol.* **37,** 911–917 CrossRef Medline
56. Livak, K. J., and Schmittgen, T. D. (2001) Analysis of relative gene expression data using real-time quantitative PCR and the $2(-\Delta\Delta C(T))$ method. *Methods* **25,** 402–408 CrossRef Medline
57. Whitehead, S. N., Hou, W., Ethier, M., Smith, J. C., Bourgeois, A., Denis, R., Bennett, S. A. L., and Figeys, D. (2007) Identification and quantitation of changes in the platelet activating factor family of glycerophospholipids over the course of neuronal differentiation by high performance liquid chromatography electrospray ionization tandem mass spectrometry. *Anal. Chem.* **79,** 8539–8548 CrossRef Medline
58. Ryan, S. D., Whitehead, S. N., Swayne, L. A., Moffat, T. C., Hou, W., Ethier, M., Bourgeois, A. J. G., Rashidian, J., Blanchard, A. P., Fraser, P. E., Park, D. S., Figeys, D., and Bennett, S. A. L. (2009) Amyloid-β42 signals Tau hyperphosphorylation and compromises neuronal viability by disrupting alkylacylglycerophosphocholine metabolism. *Proc. Natl. Acad. Sci. U.S.A.* **106,** 20936–20941 CrossRef Medline
59. Xu, H., Valenzuela, N., Fai, S., Figeys, D., and Bennett, S. A. L. (2013) Targeted lipidomics: advances in profiling lysophosphocholine and platelet-activating factor second messengers. *FEBS J.* **280,** 5652–5667 CrossRef Medline

Choline transport links macrophage phospholipid metabolism and inflammation

Shayne A. Snider, Kaitlyn D. Margison, Peyman Ghorbani, Nicholas D. LeBlond, Conor O'Dwyer, Julia R. C. Nunes, Thao Nguyen, Hongbin Xu, Steffany A. L. Bennett and Morgan D. Fullerton

J. Biol. Chem. 2018, 293:11600-11611.
doi: 10.1074/jbc.RA118.003180 originally published online June 7, 2018
